Numerical Study of Two-dimensional Vortex Street

By

Kazuhiro TSUBOI and Koichi OSHIMA

(January 10, 1985)

Summary: Two-dimensional Kármán type vortex street, which consists of two infinite parallel rows of finite area vortices, is numerically investigated using discrete vortex approximation, in which each vortex is represented by a bundle of a number of point vortices. The numerical experiment was performed for wide range of the initial conditions of the vortex street in order to make clear such characteristic features as the deformation of each vortex, the merging within each row and the formation of secondary vortex street. Also, the result showed that the initial ratio of the transverse-to-longitudinal separations of the vortices must be within 0.3 to 0.5 for stable formation of the secondary vortex street.

§1. INTRODUCTION

In nature, regular flow patterns consisting of two parallel staggered rows of vortices are frequently observed in wake of a two-dimensional bluff body when it is placed in a uniform flow. This kind of pattern is well-known as Kármán vortex street after the name of the first researcher who studied this phenomenon by replacing each vortex by a point vortex [*1*]. Complete understanding of the property of Kármán vortex street, however, has not been achieved even for the present moment [*2*]. One of the reasons of this difficulty originates in the interaction of vortices, where each vortex influences itself as well as the others. In other words, it is necessary to account for the spatial extent of vortex, particularly, for the flow field such as Kármán vortex street in which a number of vortices are closely located. This situation leads to difficulty of mathematical treatment. Method of contour dynamics has been used in order to analyze the spatial extent effect for the two-dimensional vortical flow [*3*]. This method is indeed effective for the system of few vortices, but the treatment becomes more difficult as increasing the number of vortices. In fact, the application of it to the two-dimensional vortex street has not succeeded yet.

On the other hand, the discrete vortex approximation is suitable to treat the separated vortices [*4*]–[*5*]. This approach was already carried out by Christiansen & Zabusky for the two-dimensional vortex street [*6*]. They presented the conjecture that the finite-area vortex stabilizes the system of vortices, which was confirmed by the linear stability analysis later [*7*]. Their numerical experiment, however, was performed only for six cases of geometric conditions of the vortex street. Therefore, investigation for wider range of the initial conditions is necessary.

In this paper, the interaction of the vortex street is treated using discrete vortex method, in which the continuously distributed vortical region is represented by a number of discrete vortex filaments. Therefore, the distributed vorticity is approximated as a bundle of vortex blobs. Concerning the structure of an element vortex, several models

have been proposed [8]–[9], but the simplest one that has no core and induces infinite velocity at itself is employed here. This model has, therefore, no viscous effect.

Computational scheme used is formulated in §2 based on discrete vortex method. Interaction of a single vortex row, which is an infinite row of equal-strength vortex blobs, is treated in §3. Kármán type vortex street, in which two opposite-signed single vortex rows are staggered, is investigated in §4. Particularly in §5, our attention concentrates on the transition of the vortex street, namely, the rearrangement of Kármán type vortex street.

§2. Computational Scheme

Consider the periodic flow field in the x-direction. For an infinite fow of equal-strength vortices distributed along the x-axis with the interval l, the complex potential is given by the formula [10],

$$f(z)=\frac{\kappa}{2\pi i}\log\left(\frac{\pi z}{l}\right), \tag{1}$$

$$z=x+iy. \tag{2}$$

Each vortex blob, as shown in Fig. 1, is represented by bundling a number of point vortex streets given in eq. (1). Then, the potential for this system is given as follows;

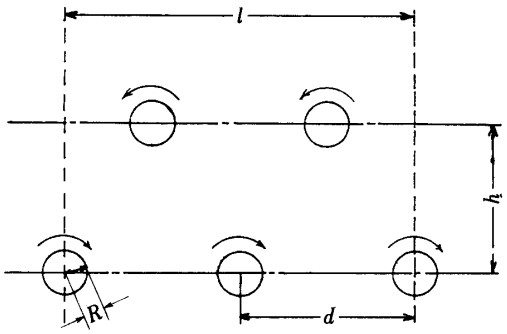

Fig. 1. Arrangement of the vortex street.

$$F(z)=\sum_{j=1}^{n}\frac{\kappa_j}{2\pi i}\log\left(\sin\frac{\pi(z-z_j)}{l}\right), \tag{3}$$

where z_j is the position of the j-th point vortex, κ_j is its strength and n is the total number of the elementary point vortices included within the interval l.

As the velocity field is given by differentiating eq. (3), the motion equations for each point vortex are;

$$\frac{d\bar{z}_k}{dt}=\sum_{\substack{j=1\\ j\neq k}}^{n}\cot\left(\frac{\pi(z_k-z_j)}{l}\right)\quad(k=1, 2, \cdots, n), \tag{4}$$

where $\bar{z}_k$ indicates the complex conjugate of z_k.

On the other hand, for the strength of a point vortex κ_j, we assume that all the point vortices within a vortex bundle have equal strengths and that they do not vary with time. Taking the total strength of the vortices consisting the vortex bundle as unity, one has,

$$|\kappa_j| = \frac{1}{N} \quad (j=1, 2, \cdots, n), \tag{5}$$

where N indicates the total number of the point vortices contained in a vortex bundle.

To solve eq. (4), the Euler's integral scheme to the second accuracy with a time step of 0.05 is employed.

§3. A Single Vortex Row

A single vortex row is considered, in which each vortex blob is arranged with the equi-distance d and has the equal circulation. In this case, there are two parameters; the distance between the neighboring vortex blobs d and the initial radius of the vortex blob R. Therefore, only one non-dimensional parameter $a=d/R$ is enough to be considered here. It is taken as $l=2a$, so that two vortex blobs are included in the computed region l.

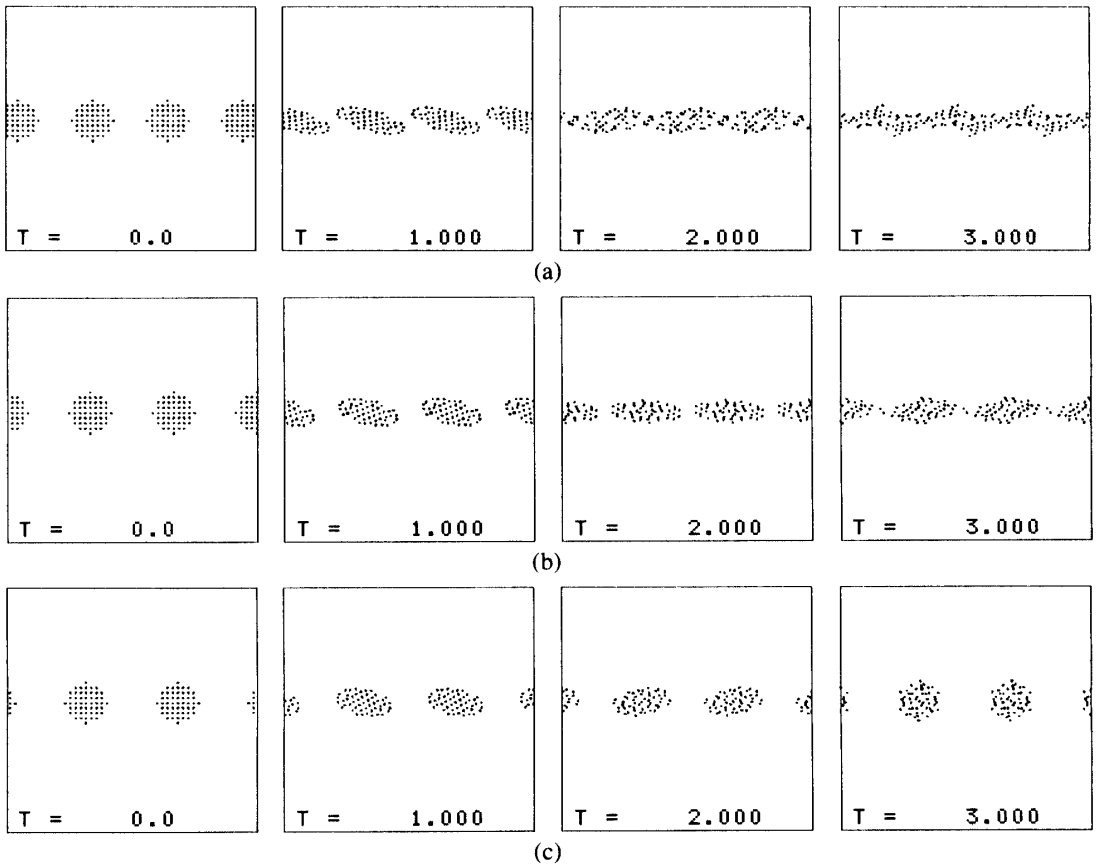

Fig. 2. Interactions of a single vortex row. This figure shows the distribution of the point vortices. (a) $a=3.6$, the complete merging occurs. (b) $a=4.0$, the critical exchange occurs. (c) $a=4.4$, no merging occurs.

Each vortex blob consists of 50 point vortices, namely $N=50$. Then the total number of point vortices in the computed region is $n=100$.

Figure 2 shows the point vortex distributions obtained for three different values of a. Complete merging of the neighboring vortex blobs occurs for $a=3.6$ (Fig. 2 (a)). Time development of this case will be discussed in detail later. In the case of $a=4.0$, each vortex blob stretches in the direction of the vortex row and a few point vortices are exchanged between the neighboring vortex blobs, as seen at $T=3.0$ (Fig. 2 (b)). Afterwards, each vortex blob changes its shape again to the initial round one. This interaction process repeats periodically. No merging of the neighbors occurs for $a=4.4$ (Fig. 2 (c)). In this case, the stretching and shrinking processes in the direction of the row repeat while each blob rotates around its own axis. Therefore, the value of a of 4.0 is regarded as the critical value for merging of the single vortex row.

§4. Kármán Type Vortex Street

Kármán type vortex street consists of two single vortex rows with the opposite-signed circulation and staggered with the separation h, as shown in Fig. 1. For this problem, there are two dimensionless parameters $a=d/R$ and $b=h/R$, which determine the geometry of the street. In the present case we also used $l=2a$, $N=50$. Therefore, the total number of point vortices within the interval l, is $n=200$. Some results are presented in Fig. 3 and Fig. 4.

In Fig. 3, the distributions of the point vortices for $a=4.4$ are shown for various values of b. In the case of $b=2.8$, each vortex blob changes its shape in the direction of the row without merging, similarly to the corresponding single vortex row (Fig. 3 (a)). In the case of smaller than 2.8, the triangular vortex blobs are formed typically seen at $T=0.5$ and 2.0 (Fig. 3 (b)). Such triangular vortices were experimentally observed for the Kármán vortex street behind a flat plate [*11*]. The initial transverse-to-longitudinal separation ratio b/a of this case, which henceforth is called the characteristic ratio, is found to be 0.32, which is close to that of Kármán vortex street. In the case with still smaller value of b, where the two rows are located very closely, each vortex blob stretches in the vertical direction of the row (Fig. 3 (c)). Such vertically stretched vortices were also found in the wake of the trailing edge of a flat plate [*11*].

Results for $a=3.6$ are shown in Fig. 4. As seen in Fig. 2 (a), for a single vortex row with this value of a, the merging of the neighboring vortex blobs occurs. Similar behaviour is found in the case with $b=2.0$ (Fig. 4 (a)). In the case of $b=1.2$ where the characteristic value of $b/a=0.33$ takes place, the triangular vortex blobs are formed again (Fig. 4 (b)), but merging of the vortex blobs does not occur. This suggests that close existence of the vortices with the opposite circulation prevents merging.

The computation is carried out for the various values of a and b. These results are summarized in Fig. 5, based on the viewpoint whether the merging within each row occurs or not. In this figure, the x-axis represents the value of b and the y-axis that of a. The symbol M means that the merging occurs at this condition. Similarly, C and N mean the critical and the non-merging conditions, respectively. The lower broken line out of two denotes the limiting values of a and b, which can be given as the initial conditions.

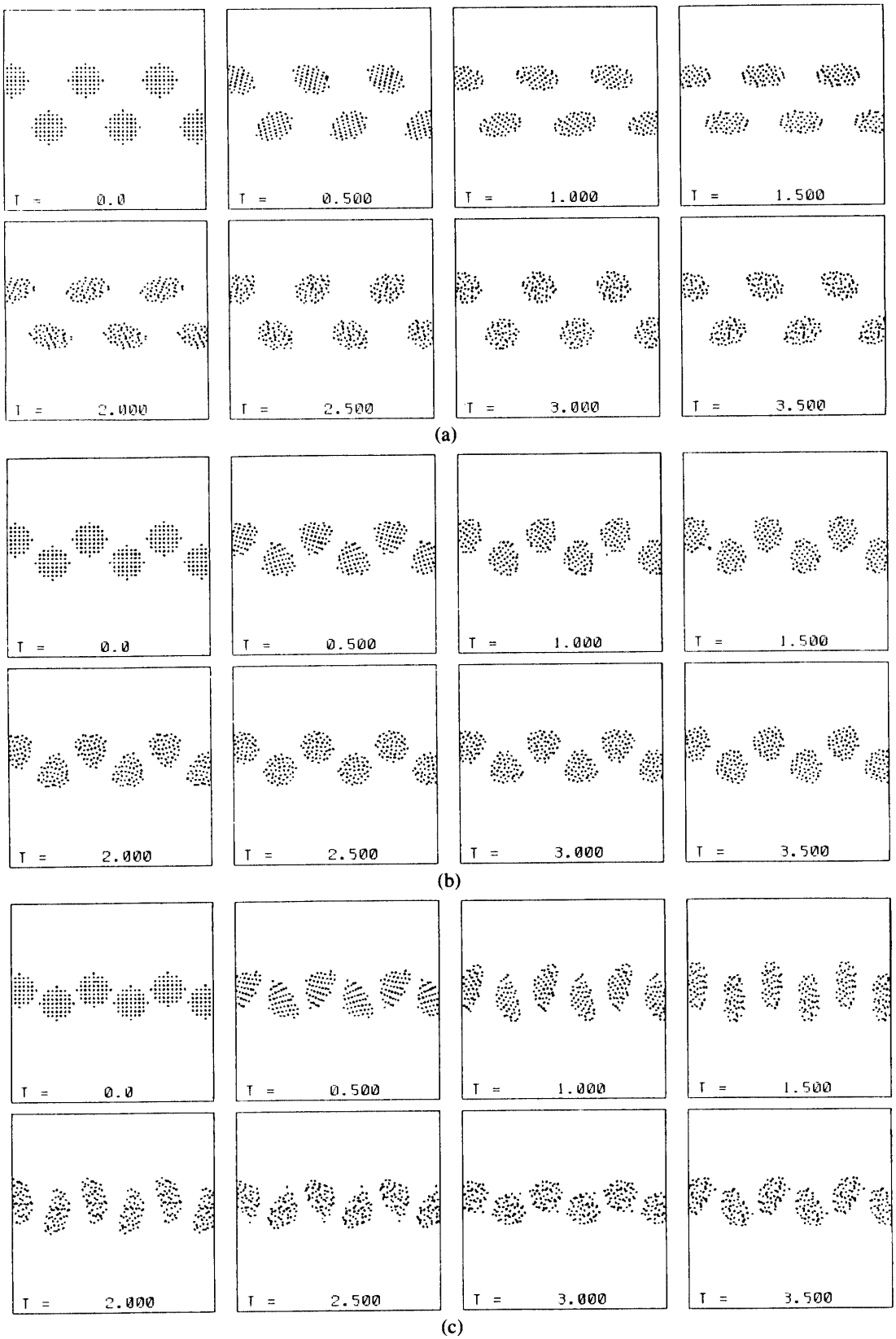

Fig. 3. Interactions of Kármán type vortex street (I). Each dot denotes the position of the point vortex. (a) $a=4.4$, $b=2.8$ (b) $a=4.4$, $b=1.4$ ($b/a=0.32$) (c) $a=4.4$, $b=0.8$.

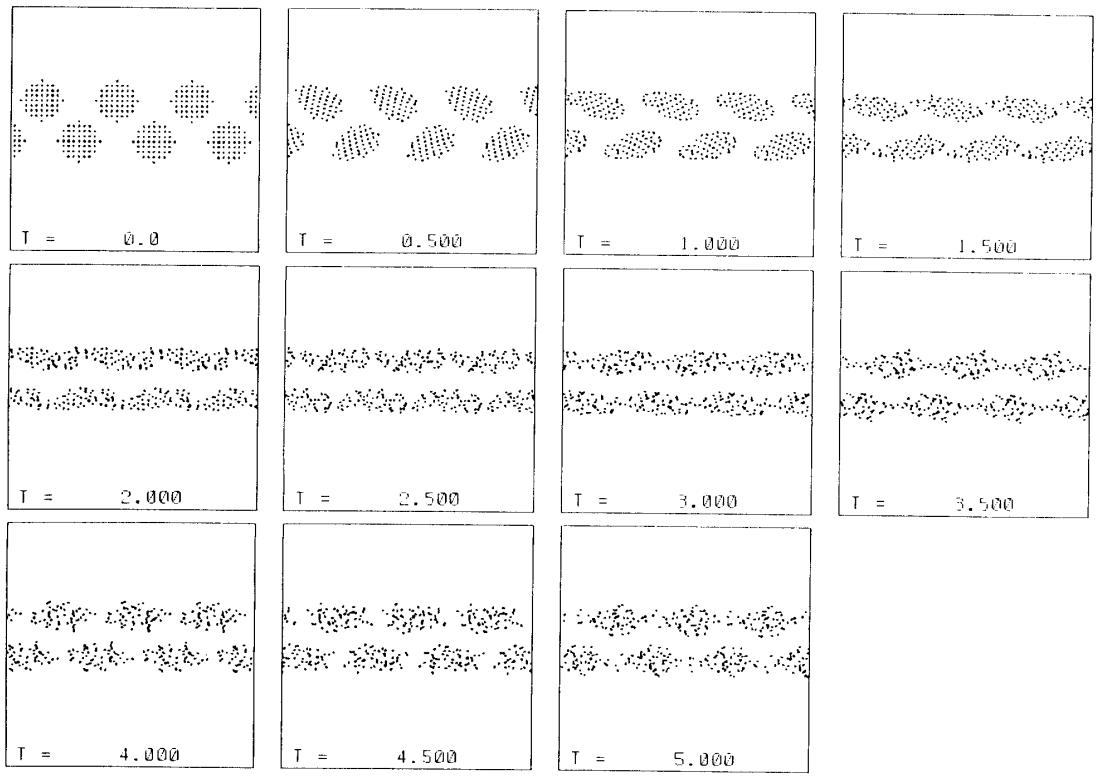

(a)

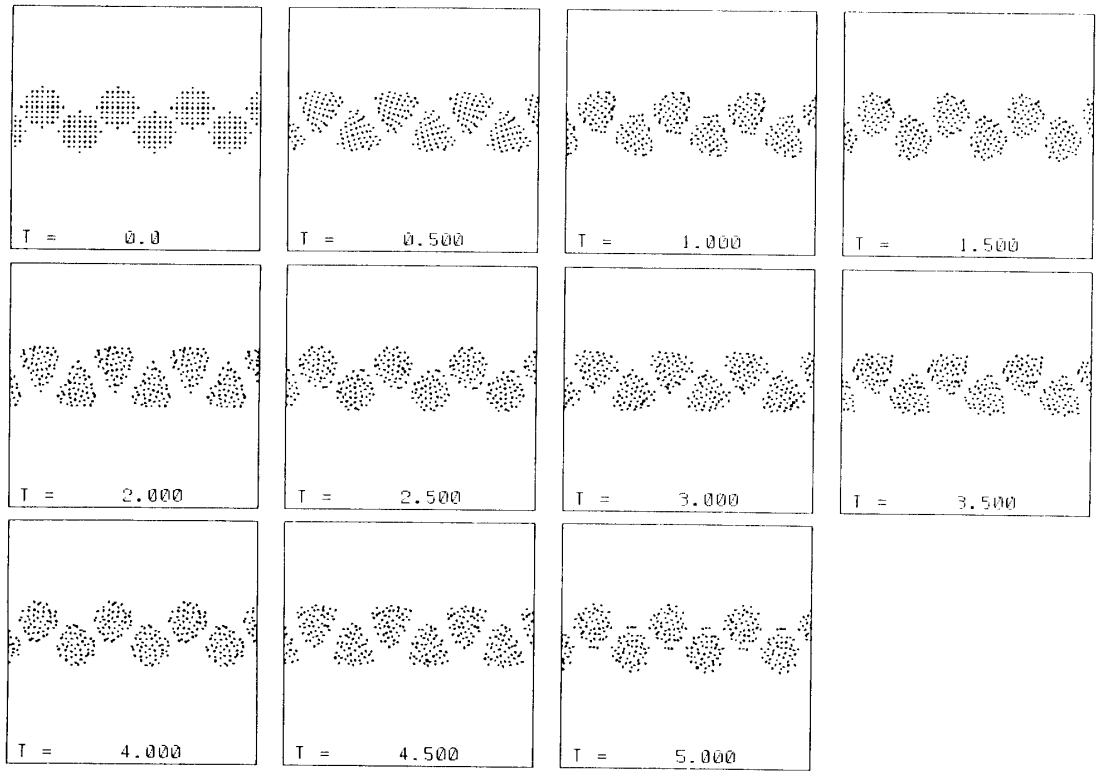

(b)

Fig. 4. Interactions of Kármán type vortex street (II). (a) $a=3.6$, $b=2.0$ (b) $a=3.6$, $b=1.2$ ($b/a=0.33$).

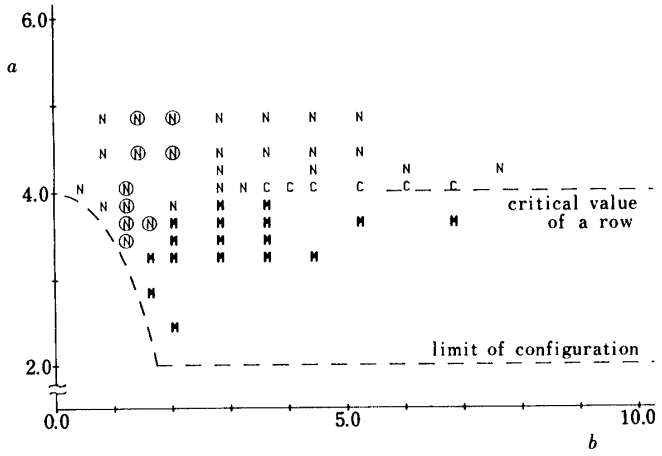

Fig. 5. The $b-a$ diagram for Kármán type vortex street. In this figure, the symbols M, C and N mean the conditions at which the merging, the critical exchange and no merging occur respectively. The open circle indecates the condition where the triangular vortex is found.

Thus, the initial condition corresponding to the lower part of this line cannot be given because of overlapping of the vortex blobs. The other broken line denotes the critical value of a for a single vortex row, as shown in §3.

Firstly, the figure shows that the critical conditions for merging of the vortex streets are almost independent of b and that they agree with the one for a single vortex row, that is, $a=4.0$. The stream lines not far from the row are almost parallel to it. Another words, the effect of the vortices is restricted within neighboring field of the row, and so-called "cat's eye" stream lines are formed. The two stream lines interfere and form the Kármán type vortex street, and each vortex row influences the other only when they are close to each other. In fact, Fig. 5 shows that the non-merging region comes down when $b<3.0$, which means that the opposite-signed vortex row prevents vortex merging, as already discussed in Fig. 4.

Nextly, let us consider the deformation of each vortex. In this figure, the open circle indicates the condition at which the triangular vortex blob is formed. These are in the range of b/a of 0.3 to 0.4. In the right side of this range where $b/a<0.3$, each vortex stretches in the vertical direction of the row; and in the left side where $b/a>0.4$, each one does so in the direction of the row. An isolated vortex region in unbounded field has a stable state with rotation which is known as "rotating V-states" [*12*]. It is suggested that the elliptic or the triangular vortex blobs found in the present simulation correspond to the stabilized state in fields with periodicity. The characters of the vortex street clarified here supports the conjecture that the spatial extent of the vortex stabilizes the vortex street.

§5. The Rearrangement of Kármán Type Vortex Street

The computations described in the previous sections make clear the condition of the merging occurrence in the Kármán type vortex street. In those computations, however,

the computed region l is taken as twice of a, so that they have only least mode for merging. In other words, such computations treat the merging of only two neighboring vortices. Though these computations with the two periodicities are effective to similate the occurrence of merging, one with the more periodic cycles is necessary for the later stage.

Figure 6 shows the time development of a single vortex row which corresponds to the succeeding stage of Fig. 2 (a), where the computed region is $8a$ and the geometric parameter a is 3.6. At $T=8.0$, the periodic structure of the vortex row breaks down and at $T=10.0$ the roll-up begins in the central position of the row. Complete formation of seven vortex blobs out of original ten vortex blobs occurs at $T=12.0$. They have no longer the same size nor the same shape. Thereafter, these vortices merge with each other and the structure of the vortex blobs grows larger and larger. As seen in this figure, eventually two large vortices are formed within the computational region.

Figure 7 shows the corresponding Kármán type vortex street, where the computational region is $8a$ and the geometric parameters $a=3.6$, $b=4.0$. The evolution of each row is similar to that in Fig. 6. Also, two larger vortices in each row are formed within the computed region. However, the arrangement of these vortices is not stable.

Figure 8 shows the same case as Fig. 7 except the value of b, where $b=2.0$. The larger-scale roll-up than in Fig. 7 occurs at $T=12.0$, because the two rows are located closer. The roll-up process forms the vortex pairs which oscillate transversely with large velocity, so that the vortex street diffuses strongly with time and eventually breaks down completely. Therefore, the stable vortex street does never exist. This process is called the dissolution mechanism [*13*] and it plays an essential role in turbulent diffusion.

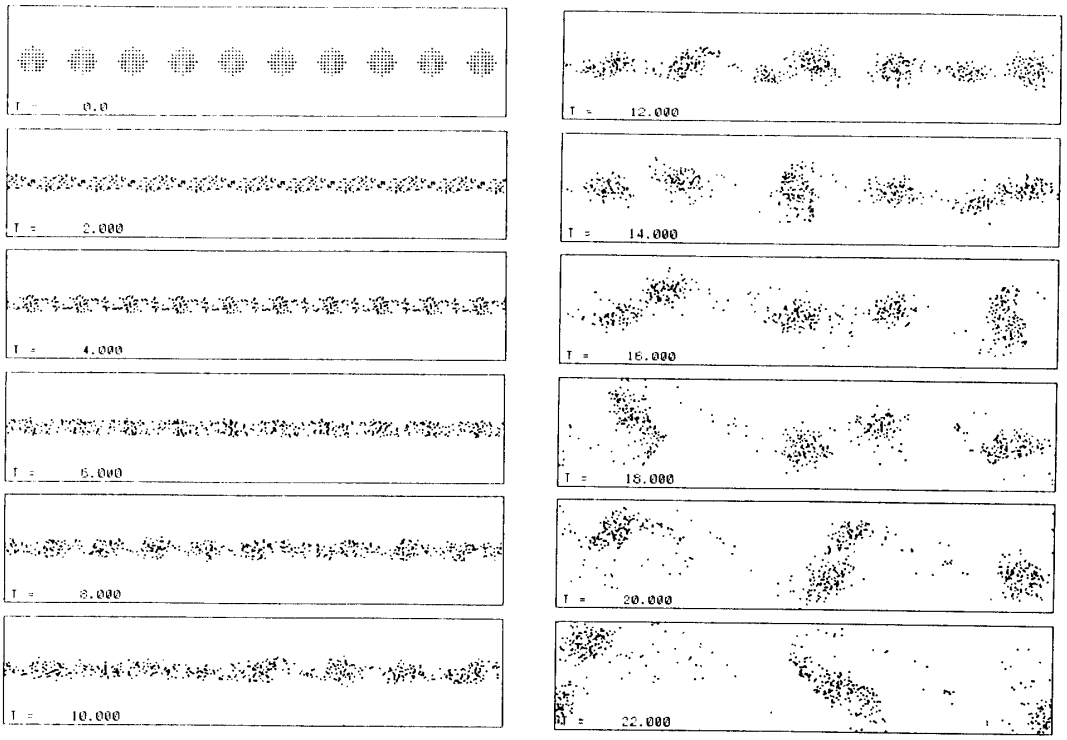

Fig. 6. Time development of a single vortex row. The conditions in this case are following: $a=3.6$, $l=8a$.

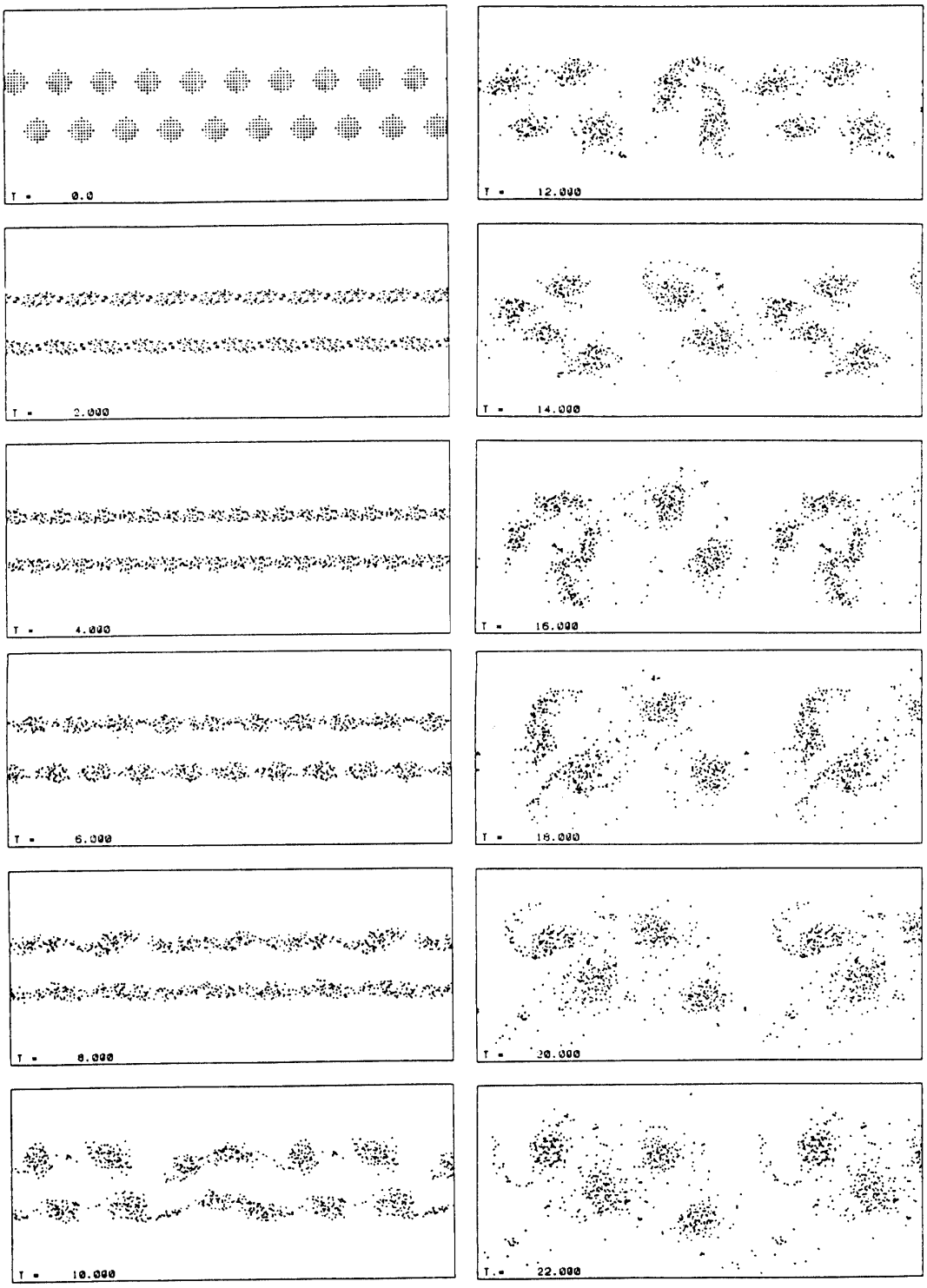

Fig. 7. Time development of Kármán type vortex street (for large b). The conditions in this case are following: $a=3.6$, $b=4.0$, $l=8a$. The resulting vortex street is not stable.

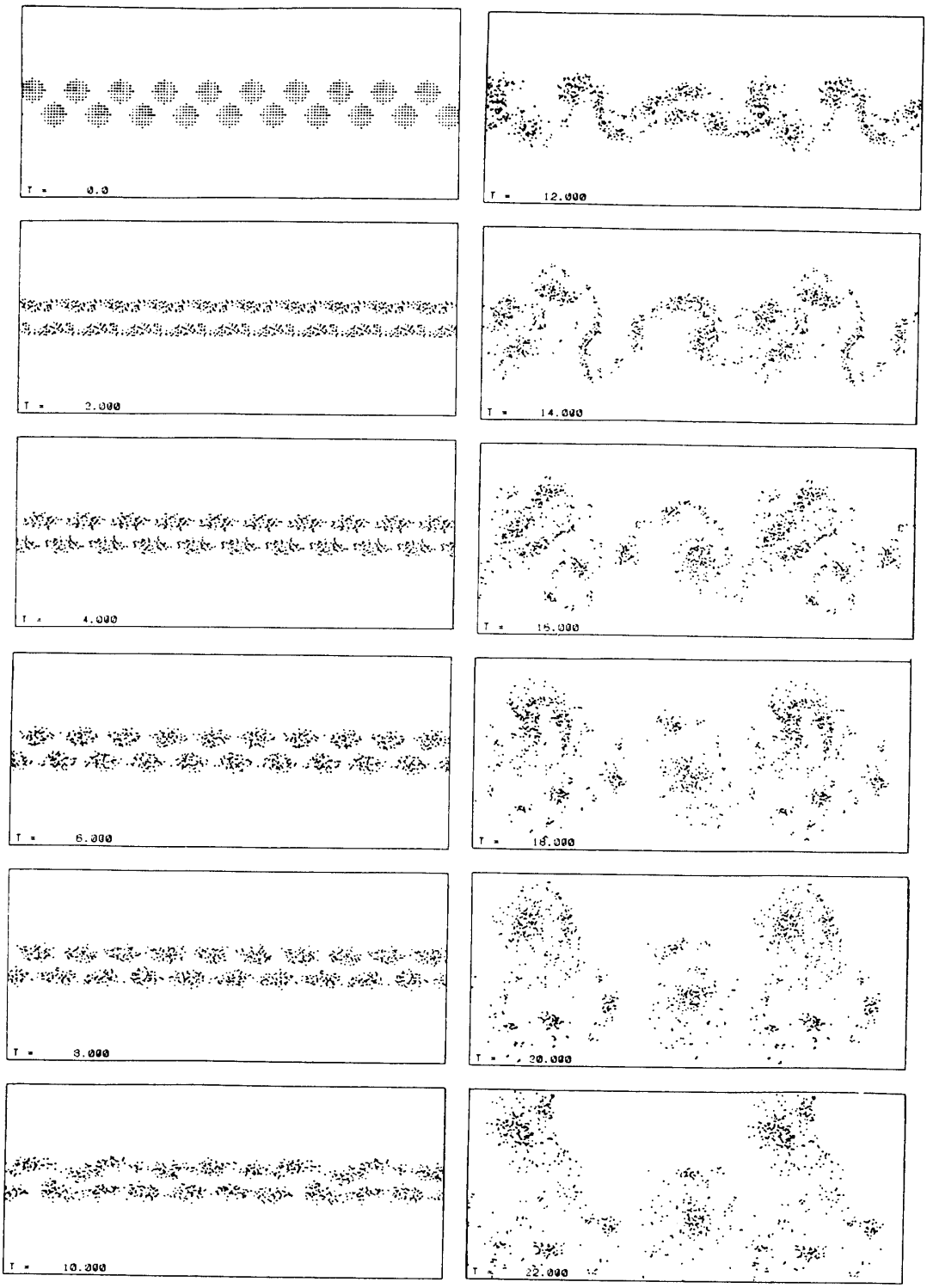

Fig. 8. Time development of Kármán type vortex street (for small b). The conditions in this case are following: $a=3.6$, $b=2.0$, $l=8a$. The dissolution mechanism is found, so that the stable secondary vortex street is not formed.

These results suggest that the formation of the secondary vortex street through the merging, namely the rearrangement, does not take place for the Kármán type vortex street with the periodic boundary condition.

As the final step, the artificial disturbance is introduced into the initial condition, the wave length of which is λ. Figure 9 (a)-(c) show the results, where the computational region is $8a$ and the wave length of the disturbance λ is $2a$. Figure 9 (a) is the case of $a=3.6$, $b=1.4$, so that the ratio $b/\lambda=0.25$. Similarly seen in Fig. 8, the dissolution mechanism is found and the width of the vortex street increases rapidly. Figure 9 (b) is the case of $a=3.6$, $b=2.5$, so that the ratio $b/\lambda=0.35$, where the stable secondary vortex street is observed. The resulting vortex street arranges four larger vortices within each row in the computing region. Figure 9 (c) is the case of $a=3.6$, $b=4.4$, so that $b/\lambda=0.61$. The vortex street grows the symmetric arrangement from the asymmetric Kármán type one. Therefore, the resulting vortex street is not stable.

Figure 10 shows the result where the computational region is $9a$ and the wave length λ is $3a$. The geometric parameters are $a=2.4$, $b=3.2$, so that $b/\lambda=0.44$. In this case, the stable secondary vortex street forms, in which three emerging vortices appear within the computing region.

Therefore, the artificial disturbance leads to the rearrangement of the vortex street only when the characteristic ratio of the resulting vortex street is $b/\lambda=0.3\sim0.5$, which is in good agreement with the result by Aref & Siggia [*13*]. The structure of the vortex street fully depends on the wave length of the initial disturbance.

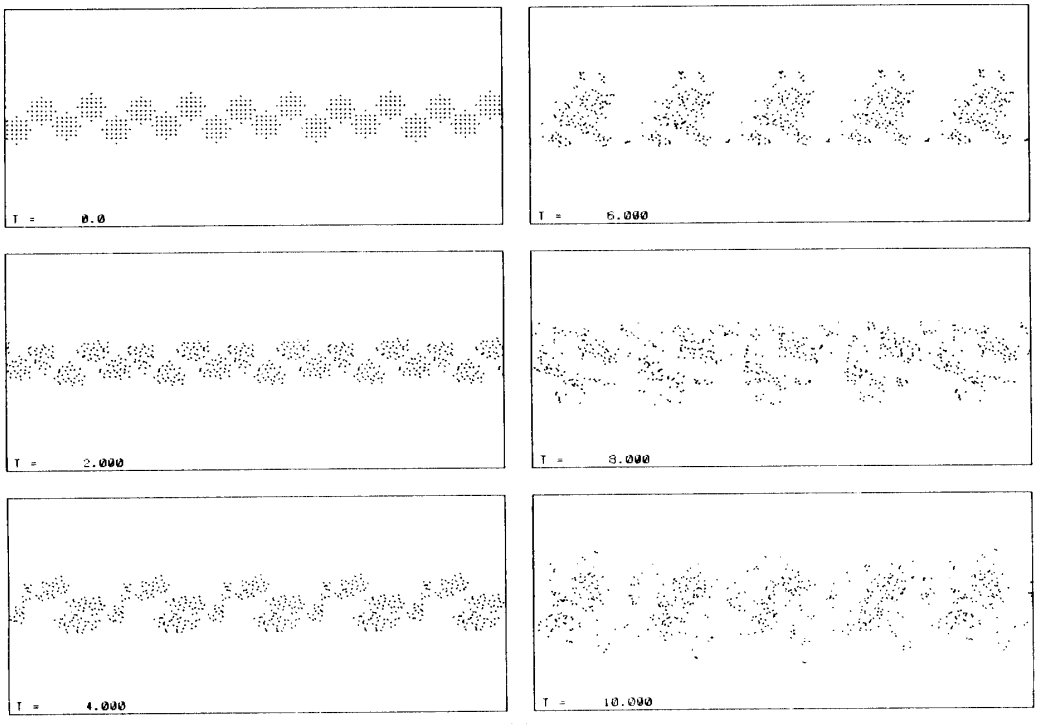

(a)

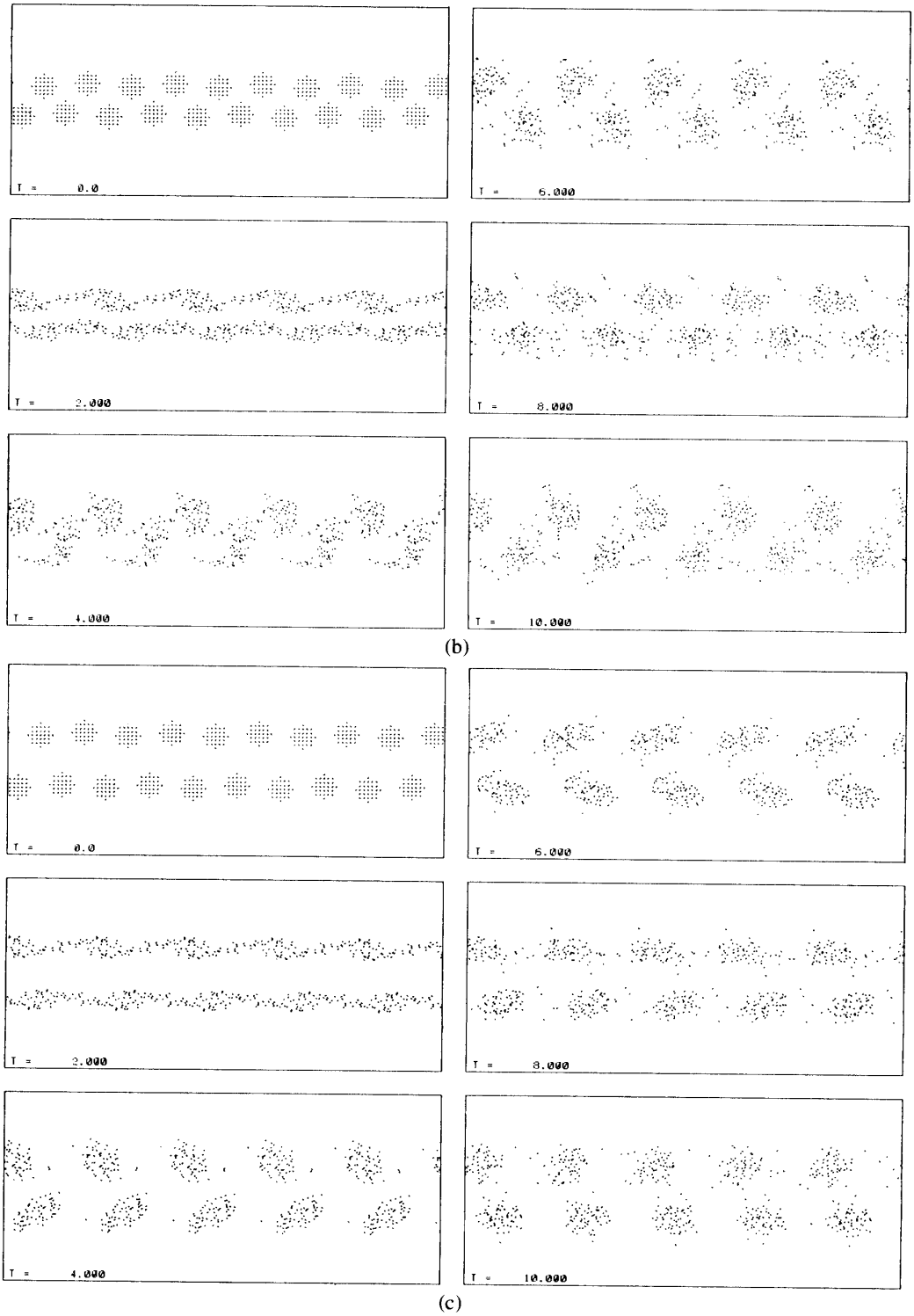

Fig. 9. Rearrangement of Kármán type vortex street (I). An artificial disturbance is introduced, the wave length of which is $\lambda=2a$. The computational region is $l=8a$. The results in three different geometric conditions are shown. (a) $a=3.6$, $b=1.4$ (b) $a=3.6$, $b=2.5$ (c) $a=3.6$, $b=4.4$. The stable secondary vortex street is formed only in the case (b).

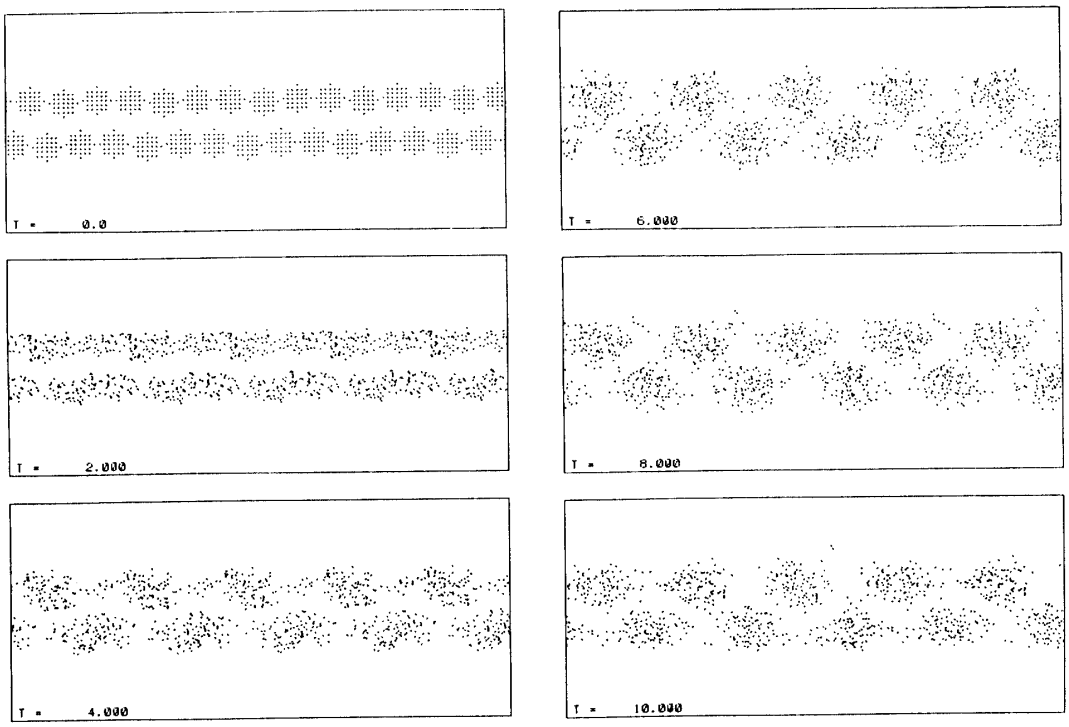

Fig. 10. Rearrangement of Kármán type vortex street (II). The wave length of the disturbance is $\lambda=3a$, and the computational region is $l=9a$. The geometric conditions are $a=2.4$, $b=3.2$. The stable vortex street is formed.

§6. Conclusion

The two-dimensional vortex streets with the finite area vortex core, in particular the Kármán type vortex streets, were investigated numerically. The finite vortex core is approximated by bundling a number of point vortices. The parameters considered are the distance between the neighboring vortices in each row a and the separation of two rows b. The following reasults are obtained.

(1) For a single vortex row which corresponds to $b\to\infty$ in the Kármán type vortex street:

No merging of vortices within each row occurs when $a>4.0$.

The exchange of the point vortices occurs when $a\sim4.0$.

The complete merging of the vortices within each row takes place when $a<4.0$.

(2) For the Kármán type vortex street:

When $b>3.0$, the critical value for the merging agrees with the case (1), that is, $a\sim4.0$.

When $b<3.0$, the critical value for the merging of a decreases, as the value of b decreases.

(3) For the deformation of the vortices in the Kármán type vortex street (the case of non-merging):

When $b/a>0.4$, the vortices stretch elliptically in the direction of the row.

When $b/a=0.3\sim0.4$, the triangular vortices are formed.

When $b/a<0.3$, the vortices stretch elliptically in the vertical direction of the row.

(4) For the rearrangement of the Kármán type vortex street:

For rearrangement of the Kármán type vortex street under the periodic boundary condition, the artificial disturbance is necessary and it determines the structure of the resulting secondary vortex street.

The secondary vortex street is formed only when its transverse-to-longitudinal ratio $b/\lambda=0.3\sim0.5$, where λ is the wave length of the artificial disturbance.

Acknowledgements

The authors wish to express their appreciation to Dr. Y. Oshima for her encouragement and many fruitful discussions.

References

[1] Lamb, H.: Hydrodynamics (6th edition), Cambridge Univ., 1932.
[2] Aref, H.: Annu. Rev. Fluid Mech. *15* (1983), 345.
[3] Zabusky, N. J., Hughes, M. H. and Roberts, K. V.: J. Comp. Phys. *30* (1979), 96.
[4] Rosenhead, L.: Proc. Roy. Soc. *A134* (1931), 170.
[5] Leonard, A.: J. Comp. Phys. *37* (1978), 289.
[6] Christiansen, J. P. and Zabusky, J.: J. Fluid Mech. *61* (1973), 219.
[7] Saffman, P. G. and Schatzman, J. C.: J. Fluid Mech. *117* (1982), 171.
[8] Chorin, A. J.: J. Fluid Mech. *57* (1973), 785.
[9] Kuwahara, K. and Takami, H.: J. Phys. Soc. Japan *34* (1973), 247.
[10] Imai, I.: Fluid Mechanics Part I, Shookabo Pub. (1978) (in Japanese).
[11] Taneda, S.: J. Phys. Soc. Japan *13* (1958), 418.
[12] Deem, G. S. and Zabusky, N. J.: Phys. Rev. Lett. *40* (1978), 859.
[13] Aref, H. and Siggia, E. D.: J. Fluid Mech. *109* (1981), 435.